Pollution, 6(1): 171-184, Winter 2020
DOI: 10.22059/poll.2019.289061.679
Print ISSN: 2383-451X Online ISSN: 2383-4501
Web Page: https://jpoll.ut.ac.ir, Email: jpoll@ut.ac.ir

Removal of Methyl Orange Dye from Aqueous Solution by a Low-Cost Activated Carbon Prepared from Mahagoni (*Swietenia mahagoni*) Bark

Ghosh, G. C.[*], Chakraborty, T. K., Zaman, S., Nahar, M. N. and Kabir, A. H. M. E.

Department of Environmental Science and Technology, Jashore University of Science and Technology, P.O.Box 7408, Jashore, Bangladesh

Received:17.09.2019 Accepted: 23.11.2019

ABSTRACT: This study utilized *Swietenia mahagoni* bark–a wood processing industry waste, for the preparation of activated carbon, and then investigated for the removal of methyl orange (MO) dye by the *Swietenia mahagoni* bark activated carbon (SMBAC). The effect of pH (3–10), adsorbent dose (1–30 g/L), initial MO dye concentration (10–100 mg/L), and contact time (1–240 min) were evaluated. The surface morphology of the SMBAC was characterized by using fourier transform infrared spectroscopy (FTIR) and scanning electron microscopy (SEM). Maximum removal efficiency of MO by SMBAC was 92%, when initial MO dye concentration was 10 mg/L, pH 3.0, adsorbent dose 10.0 g/L and 120 min equilibrium contact time. The adsorption data fitted well with the Freundlich (R^2=0.997) and Halsey (R^2=0.997) isotherm models than the Langmuir (R^2=0.979) model, and express the multilayer adsorption on heterogeneous surface. The maximum adsorption capacity was 6.071 mg/g. The kinetics data were fitted well to pseudo-second order model (R^2=0.999) and more than one process were involved during adsorption mechanism but film diffusion was the potential rate controlling step. The study results showed that SMBAC adsorbed MO effectively, and could be used as a low cost potential bioadsorbent for the removal of anionic dyes in wastewater treatment.

Keywords: Adsorption; Isotherms; Kinetics; Biosorbent.

INTRODUCTION

Many textile, printing, plastic, dye synthesis, pulp and paper mill, leather, electroplating, food, cosmetic, pigments, petroleum, rubber, pesticide etc. industries that use dyes release a huge amount of highly coloured effluent in their wastewater. The presence of very small amounts of dyes in water affects photosynthetic activity by preventing light penetration and upset the biological metabolism processes in aquatic life (Garg et al., 2004). Dye also produces micro toxicity for fish and other aquatic organisms by chelating metal ion (Babel & Kurniawan, 2003; Garg et al., 2004). Moreover, some of the dyes and their degradation products cause skin irritation, eye burn, diarrhea, cancer as well as mutagenic or carcinogenic influences on living organisms including human (Aksu, 2005; Nasuha & Hameed, 2011). MO is an organic, acidic, anionic and water soluble azo dye, extensively found in wastewater which has been released from research laboratory, food, textile, paper and printing industries, pharmaceutical, leather, cosmetic, plastic and dye manufacturing industries (Gong et al., 2005; Cheah et al., 2013). MO can causes different types of health hazard by damaging the function of kidneys, liver,

[*] Corresponding Author, Email: gopales8@hotmail.com

central nervous system, brain and reproductive system (Özcan & Özcan, 2004; Cheah et al., 2013). Synthetic origin, aromatic ring structure, oxidation reaction and azo link (−N=N−) makes the MO dye difficult to degrade (Aksu, 2005; León et al., 2016). Different techniques have been used to remove dyes from wastewater including, coagulation/flocculation, membrane separation, oxidation/ozonation, reverse osmosis , photocatalysis, ultrafiltration, electrochemical, adsorption and biosorption (Panda et al., 2009; Liu et al., 2013; Pathania et al., 2013; Hasan & Hammood, 2018). Among them, biosorption has become the most popular technique because of its effectiveness, operational simplicity, low cost and low energy requirements (Royer et al., 2009). On the other hands, activated carbon/modified activated carbon is consider as an feasible adsorbent for pollutant removal and largely used due to its extensive surface area, significant porous space, high removal efficiency, different functional groups on adsorbent surface, fast adsorption kinetics, chemical characteristics and instinctiveness of regeneration (Chen et al., 2010; Halim et al., 2010; Ghasemian & Palizban, 2016). Recently, many waste materials or by-products have been investigated as adsorbents for removing dyes from water; some examples include activated carbon of coffee grounds (Rattanapan et al., 2017), chitosan (Saha, et al., 2010), commercial granular activated carbon (León et al., 2016), *Eucalyptus sheathiana* bark biomass (Afroze et al., 2016), pine bark (Leitch et al., 2006), bark powder of tree (DIM, 2013), bentonite and activated carbon (Bellifa et al., 2017), finger citron residue based activated carbon (Gong et al., 2013), modified carbon coated monolith (Cheah et al., 2013), *Phragmites australis* activated carbon (Chen et al., 2010), calcined Lapindo volcanic mud (Jalil et al., 2010), ultrafine coal powder (Zhuannian et al., 2009), melon husk (Olajire et al., 2015), modified bentonite (Wang et al., 2014), electrospun activated carbon fibers (Sun et al., 2014), yam leaf fibers (Vinoth et al., 2010) etc. Mahagoni tree (*Swietenia mahagoni*) is naturalised in southern Florida, USA and now widely cultivated in other areas of the tropics. Mahagonies bark used as a medicine for the treatment of hypertension, diabetes, malaria, epilepsy, anemia, diarrhea, dysentery, fever, loss of appetite, and toothache (Panda et al., 2010). Rubiadin dye prepared from this tree bark (Haque et al., 2013). Mahagoni tree bark is a wood processing industry waste selected in this work due to its availability, abundantly, inexpensive and environmental friendly as way to substitute or supplement commercially available adsorbents. The objective of this study was to investigate the applicability of SMBAC for removal of MO from aqueous solution with variation of experimental conditions (pH, contact time, adsorbent dose, and initial dye concentration). The adsorption isotherms and kinetics were also investigated.

MATERIALS AND METHODS

The analytical grade MO was purchased from sigma-Aldrich, USA. The chemical formula of MO is $C_{14}H_{14}N_3NaO_3S$, molecular weight 327.34 g/mol, pH range 3–4.4, purity 85% and used this adsorbate without further purification. All the chemicals were analytical grade and double distilled water were used for performing the experiments. To prepare MO stock solution (400 mg/L), an appropriate amount of MO was dissolved in double distilled water. Desired working solution of MO was prepared from the stock solution by diluting with double distilled water. The pH of experiment solution was adjusted by adding 0.1 N HCl / 0.1 N NaOH, and pH were measured by using a digital pH meter (EZdo 6011, Taiwan). The concentration of MO in experimental solution was measured by UV-visible spectrophotometer (HACH DR 3900, USA) at 464 nm wavelength. The instrument was re-calibrated at the

beginning of each set of analysis. Calibration standards run once each five samples and compared. If the value varies from the known value >5%, instrument was recalibrated.

Mahagoni (*Swietenia mahagoni)* bark was collected from a sawmill located in Jashore, Bangladesh. After collection, it cut into small pieces (5 inches long) and washed with tap water to remove dirt and colour from its body. Then further washed with double distilled water and dried in an oven (Labtech LDO-150F, Korea) at 80°C for 24 h, cooled in room temperature. The bark was soaked in 0.1N NaOH solution for 24h to remove excess colour, after that dried again in an oven at 80°C for 24 h, carbonized into a muffle furnace (SXT-10, Shanghai Shuli Instrument and Meters Co., Ltd.) at 200^{o}C for 15 min. Then carbonized charcoal was wash with double distilled water and further dried in an oven at 80°C for 24 h, crushed by a mortar and pestle, and 0.5 to 1.0 mm size particles were collected through sieved. Finally, SMBAC was stored in airtight borosilicate glass bottles and, used for experiments as needed. The surface morphology of fresh SMBAC was characterized by FTIR spectrometer (FTIR-8400S Shimadzu, Japan) and field emission scanning electron microscope (FESEM) (JEOL JSM 7600F, Japan), respectively.

Adsorption of MO onto SMBAC was conducted by batch experiments in 500 mL beakers. The adsorbent was added into the 200 mL working solution with desired MO dye concentration and stirred at 200 rpm for 120 min equilibrium contact time at room temperature (25±2^{0}C). The other experimental conditions; pH (3–11), adsorbent dose (1-30 g/L) and initial MO dye concentration (10–100 mg/L) were studies. Every experiment was performed by a Jar-test instrument (JLT4, VELP Scientifics, Italy). After completion of each experiment, suspension was taken from the beaker and filtered through Whatman® glass microfiber filters (grade GF/B) in order to removing adsorbent particles. Duplicate experiments were conducted and mean values were applied. The amount of MO adsorption at equilibrium and percentage of removal were calculated by using Equation (1) and Equation (2), respectively:

$$q_e = \frac{(C_0 - C_e)V}{m} \quad (1)$$

$$R(\%) = \frac{(C_0 - C_e)}{C_0} \times 100 \quad (2)$$

where q_e is the amount of adsorbate adsorbed at time t (mg/g), C_0 and C_e are initial and equilibrium adsorbate concentration in mg/L, respectively. V is the volume of the solution (L) and m is the mass of adsorbent (g).

The isotherm experiments were conducted with different initial MO concentration (10, 20, 30, 50 and 100 mg/L) with 10 g/L adsorbent dose and stirred at 200 rpm for 120 min equilibrium contact time at room temperature (25±2^{0}C) with optimum pH 3. Here, three equilibrium adsorption isotherm models (The Langmuir, Freundlich and Halsey) were used. Langmuir isotherm assumes the finite sites are distributed homogeneously all over the surface of adsorbent, where monolayer adsorption occurred (Langmuir, 1917).The linear form of Langmuir isotherm is presented in Equation (3):

$$\frac{C_e}{q_e} = \frac{1}{q_{max}b} + \frac{C_e}{q_{max}} \quad (3)$$

where C_e is the equilibrium concentration (mg/L), q_e is the adsorption capacity at equilibrium (mg/g), q_{max} is the maximum adsorbate uptake per unit mass of adsorbent (mg/g) and b is Langmuir constant (L/mg). The Langmuir parameters also obtained from the Ce/q_e versus Ce plotting**.** The Langmuir isotherm can also be described by an equilibrium parameter (R_L) which represents the adsorption system is favorable or unfavorable.

Equilibrium parameter (R_L) is presented in Equation (4):

$$R_L = \frac{1}{1+bC_0} \quad (4)$$

The adsorption process as a function of R_L may be described as $R_L > 1$; unfavorable, $R_L = 1$; Linear, $0 < R_L < 1$; favorable and $R_L = 0$; irreversible.

Freundlich isotherm is an empirical equation describes the multilayer adsorption on heterogeneous surfaces of adsorbent. Where, adsorbent active sites are exponentially distributed and adsorption rate of adsorbent is not constant for a given concentration (Freundlich, 1906). The linear form of Freundlich model is presented in Equation (5):

$$\log q_e = \log K_F + 1/n . \log C_e \quad (5)$$

where K_F and n are Freundlich constant that represents adsorption capacity and adsorption intensity, respectively. Therefore, a plot of $logq_e$ against $logC_e$ gives a straight line; K_F and $1/n$ are determined from the intercept and slope. Values of n, between 1 and 10 indicate a favorable adsorption process, while higher K_F value indicates an easy uptake of dye from the solution.

Halsey isotherm model describes the multilayer adsorption at a relative distance from the surface (Song et al., 2014). The linear form of this equation is in Equation (6):

$$\log q_e = \frac{1}{n_H} logK_H - \frac{1}{n_H} \log C_e \quad (6)$$

where K_H and n_H are the Halsey constants can be obtain respectively from the intercept and slope of plot $logq_e$ versus $logC_e$.

For the adsorption kinetics experiment, 10 g/L adsorbent dose was added into 350 mL working solution of 20 mg/L MO dye at optimum pH 3 and starring speed 200 rpm at room temperature (25 ± 2^0C). The samples were collected from the experimental solution after selected time interval (1, 2, 3, 5, 7, 10, 30, 60, 90, 120, 150, 180, 210 and 240 min), and then filtered for MO analysis in the samples. Experimental data generated from MO adsorption tests using SMBAC were evaluated to understand the mechanisms and dynamics of the adsorption process. The Lagergren pseudo-first order model and Ho's pseudo-second order model were used to know the kinetics behavior of MO dye adsorption onto SMBAC. Whereas, the Weber and Morris intraparticle diffusion model and Boyed model were used to investigate the mechanism and potential rate controlling step that are involved in adsorption process. The Lagergren pseudo-first order model describes the adsorption rate of adsorbate, which is directly proportional to the number of available vacant space on adsorbent surface (Jalil et al., 2010) and presented in Equation (7):

$$\frac{dq_t}{dt} = k_1 (q_e - q_t) \quad (7)$$

Integrating the Equation (8) with limit; $t = 0$ to $t = t$ and $q_t = 0$ and $q_t = q_t$ and the linear form of Lagergren pseudo-first order model is shown in Equation (8):

$$\log (q_e - q_t) = \log (q_e) - \frac{K_1}{2.303} t \quad (8)$$

where K_1 is the pseudo-first order rate constant (min^{-1}), q_e and q_t are the amount of adsorbate adsorbed (mg/g) at equilibrium and time, t. K_1 and q_e can be obtain respectively from the slope and intercept of a linear plot of $log(q_e - q_t)$ versus t.

Ho's pseudo-second order kinetic model assumes that adsorption capacity of adsorbate is proportional to the square of the number of available vacant space on adsorbent surface (Ho & McKay, 2000), and expressed in Equation (9):

$$\frac{dq_t}{dt} = k_2 (q_e - q_t)^2 \quad (9)$$

Integrating the Equation (10) with limit;

$t = 0$ to $t = t$ and $q_t = 0$ and $q_t = q_t$, the linear form of Ho's pseudo-second order model was obtained and present in Equation (10):

$$\frac{t}{q_t} = \frac{1}{K_2 q_e^2} + \frac{1}{q_e}(t) \quad (10)$$

where K_2 is the pseudo-second order rate constant (g/mg/min), by replacing the $K_2 q_e^2$ by H in Equation (11), we have the Equation (11):

$$\frac{t}{q_t} = \frac{1}{H} + \frac{1}{q_e}(t) \quad (11)$$

where H is the initial adsorption rate (mg/g/min); constant (H) and q_e can be obtained from the intercept and slope of a linear plot oft/q_t versus t.

The Weber and Morris model indicates the presence of intraparticle diffusion of adsorbate in adsorbent surface during adsorption process (Weber & Morris, 1963). The intraparticle diffusion model is expressed in Equation (12):

$$q_t = K_{diff.} t^{0.5} + C \quad (12)$$

where $K_{diff.}$ is the intraparticle diffusion rate constant (mg/g $min^{0.5}$), that can be calculated from the slope of a linear plot of q_t versus $t^{0.5}$, and C is intercept, that represent the thickness of boundary layer. If the linear plot pass through the origin, with no intercept then intraparticle diffusion only the rate limiting step. Otherwise not only intraparticle diffusion but also other diffusion mechanism will also be involved during adsorption process (Hameed et al., 2009). On the other hands, if the plot represents multi-linearity, then combine process (external and internal diffusion) controlled the process and many steps are involved (Srivastava et al., 2006).

Boyd model (Cáceres-Jensen, 2013) applied to determine the step which is engaging during adsorption mechanism. The Boyd model can be expressed as Equation (13):

$$F = \frac{q_t}{q_e} = 1 - \frac{6}{\pi^2}\exp(-Bt) \quad (13)$$

where B_t is the function of F, and F is the fraction of solute adsorbed at different times, t. The B_t values can be calculated at different contact times, t, by using the Equation (14):

$$B_t = -0.4977 - \ln(1 - F) \quad (14)$$

Boyd model can be obtained by B_t versus t plotting. If the Boyd linear plot pass through the origin then intraparticle diffusion is predominates otherwise film diffusion is the rate limiting step (Nethaji et al., 2013).

RESULTS AND DISCUSSION

The percentage transmission for various wave numbers and the adsorption bands were identified in the spectra of SMBAC and presented in Fig. 1(a),

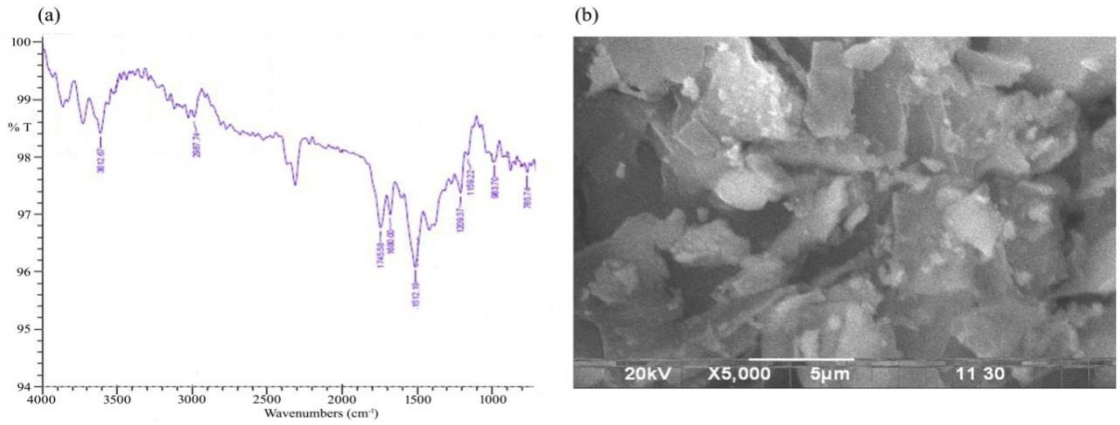

Fig. 1. (a) FTIR spectra of SMBACand (b) SEM image of SMBAC (magnification=5000x).

A 'fingerprint region' was found after 1700 cm^{-1}, where adsorption was barely attributed. The two prime peak were found at 3612.67 cm^{-1} (cellulose contain –OH group) and 2987.74 cm^{-1} (lignin, cellulose, hemicellulose contain C-H group) band, and respectively (Panda et al., 2009; Salazar-Rabago et al., 2017). The 1745.58 cm^{-1} peak assigned to carboxyl acid groups and different types of hemicellulose (Panda et al., 2009; Salazar-Rabago et al., 2017). The peak at 1512.19 cm^{-1} and 1680.00 cm^{-1} indicates that C=C group with lignin was present. The other peak at 1209.32, 1159.22, 983.70 and 765.74 cm^{-1} reflect the stretching vibration C-H, C-O, C=O and C-C, respectively (Fig. 1(a)). Similar IR spectrum and functional groups found by several author (Cheah et al., 2013; Zhao et al., 2017; Yu et al., 2018). So, above functional groups were effective for adsorption of MO by SMBAC. The surface structure of adsorbent was analyzed by SEM. The irregular, rough and porous surface was found on the adsorbent surface (Fig. 1(b)), also promote MO adsorption onto SMBAC.

The removal percentages and adsorption capacity of MO dye by SMBAC was carried out with contact time variation (1 to 240 min). The maximum MO removal efficiency of 85% and adsorption capacity of 1.72 mg/g was found at 120 min contact time (Fig. 2(a)). The adsorption processes follow two steps. In the first step, 69% removal occurred within first ten minute (Fig. 2(a)) due to available vacant space on adsorbent surface with high concentration of MO. The removal efficiency was slow in second steps for lacking of vacant space of adsorbent surface and lower MO dye concentration (Han et al., 2007), and finally equilibrium was reached at 120 min (Fig. 2(a)), where all active sites were saturated and no significant change was observed after this equilibrium time. In dye adsorption process, pH plays an important role in the chemistry of dye ionization and adsorbent surface charged modification (Ghasemian & Palizban, 2016). As shown in Fig. 2(b), the removal percentage of MO was high at pH 3 and removal percentages decreased from 85 to 24% with increasing pH from 3 to 10. At low pH, the surface charge of adsorbent become positive due to protonation, so the Van der Waals interactions and electrostatic attraction between the anionic MO dye and the positive change of adsorbent surface consequently increased MO removal.

As the pK_a of MO is 3.5, so above the pH 3.5 the MO dye will have a negative charged (sulfonic group in negative charge form), as a result the electrostatic repulsion between aromatic ring of anionic MO dye and negatively charged adsorbent reduce MO removal efficiency (León et al., 2016). Similar result was found during MO adsorption by coffee grounds activated carbon (Rattanapan et al., 2017).

Adsorbent dose is very important because it not only determine the adsorption capacity of an adsorbent at a fixed initial dye concentration but also determine the treatment cost of solution per unit volume. The MO removal percentage was increased from 34 to 98% due to increasing the adsorbent dose from 1 to 30 g/L (Fig. 3(a)), the possible causes are large surface area and more available unsaturated active site for adsorption at higher adsorbent dose. Whereas, the adsorption capacity of MO by SMBAC was decreased from 6.87 to 0.65 mg/g with increasing adsorbent dose from 1 to 30 g/L (Fig. 3(a)) due to particle aggregation of SMBAC at higher dose, which reduce the available surface area and results in increase competition or overlapping between the MO dye molecules (Han et al., 2007). However, the optimum dose of SMBAC directly depends on MO concentration, higher SMBAC dose requires for removal of higher MO concentration (Panda et al., 2009). Adsorption capacity and removal

efficiency of MO dye by SMBAC was carried out with different initial dye concentration ranging from 10 to 100 mg/L. The adsorption capacity of SMBAC was increased from 0.92 to 5.32 mg/g with increasing MO dye concentration from 10 to 100 mg/L at fixed SMBAC dose of 10 g/L (Fig. 3(b)).

This may be due to the high interaction between MO dye and SMBAC that enhance the significant driving force to transfer high mass of MO between the liquid to solid phase in aqueous solution (Senthil et al., 2011). Whereas, the removal efficiency of SMBAC was gradually deceased (92 to 53%) due to increase MO dye concentration (Fig. 3(b)) because all active sites of adsorbent saturated after certain MO dye concentration at constant adsorbent dose, and excess MO remain unadsorbed in the solution.

Adsorption isotherm not only represents the information regarding the adsorption capacity of adsorbent but also describe the interaction between adsorbate and adsorbent during adsorption process (Malkoc & Nuhoglu, 2007).

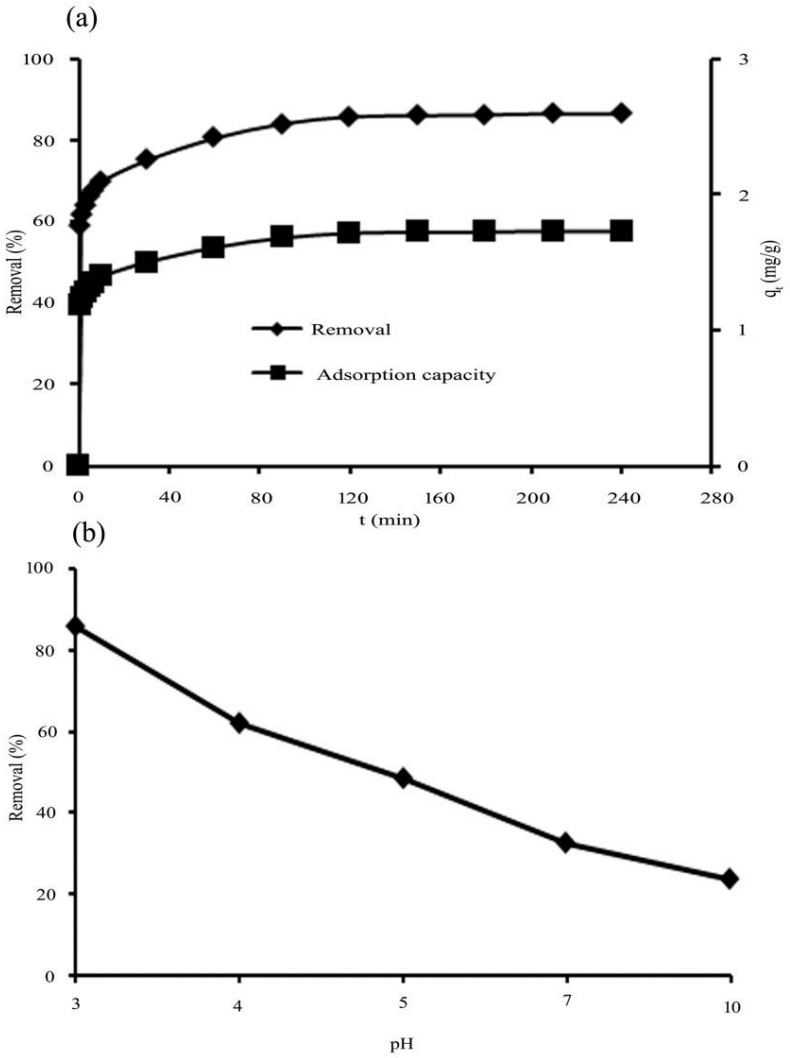

Fig. 2. Effect of (a) contact time, and (b) pH on removal of MO by SMBAC [Experimental condition: adsorbent dose (10 g/L), rotation speed (200 rpm) and temperature (25±2^{o}C), initial MO dye concentration (20 mg/L)].

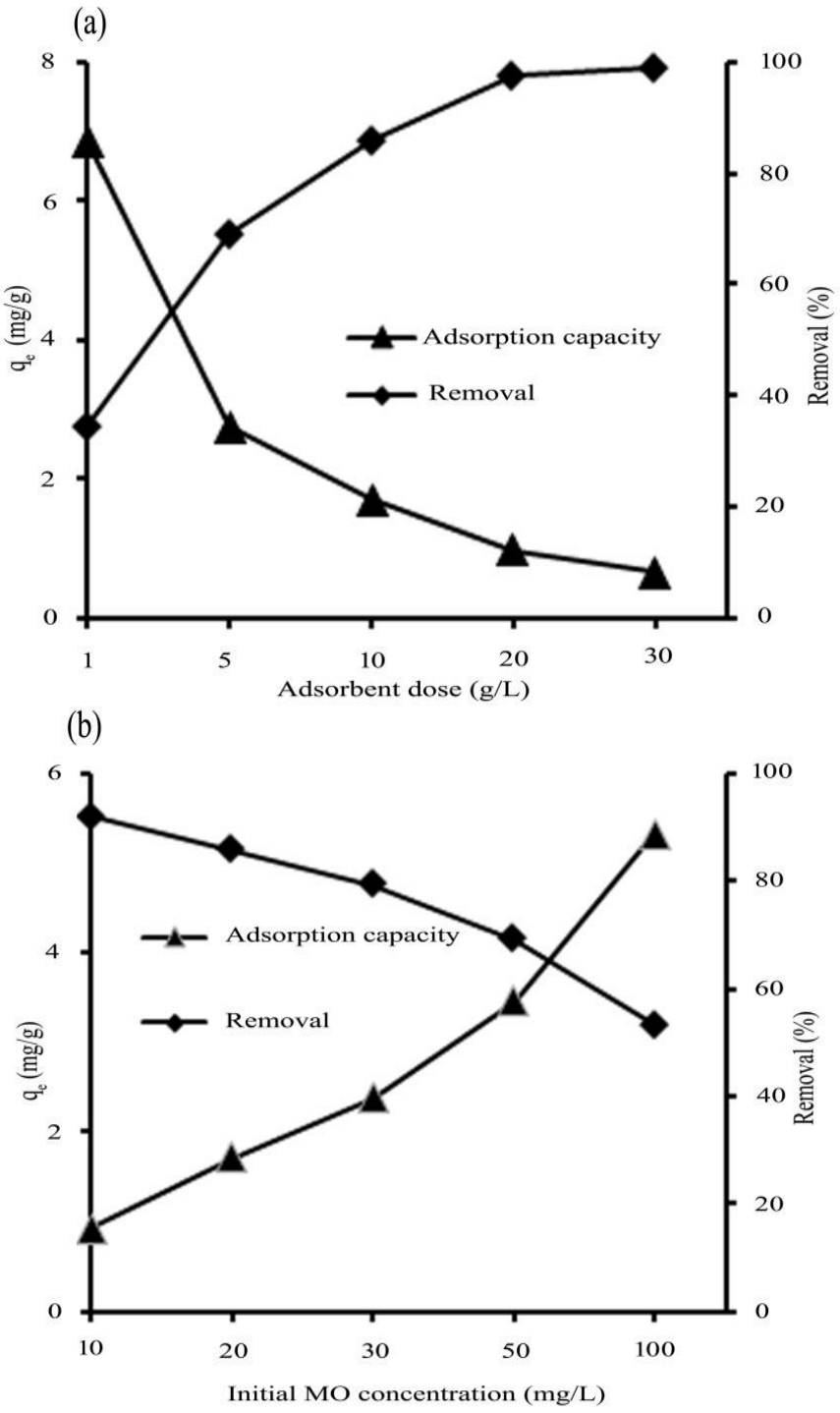

Fig. 3. Effect of (a) adsorbent dose, and (b) of initial MO concentration on removal of MO by SMBAC [Experimental condition: pH (3), contact time (120 min), rotation speed (200 rpm) and temperature (25±2^{o}C)].

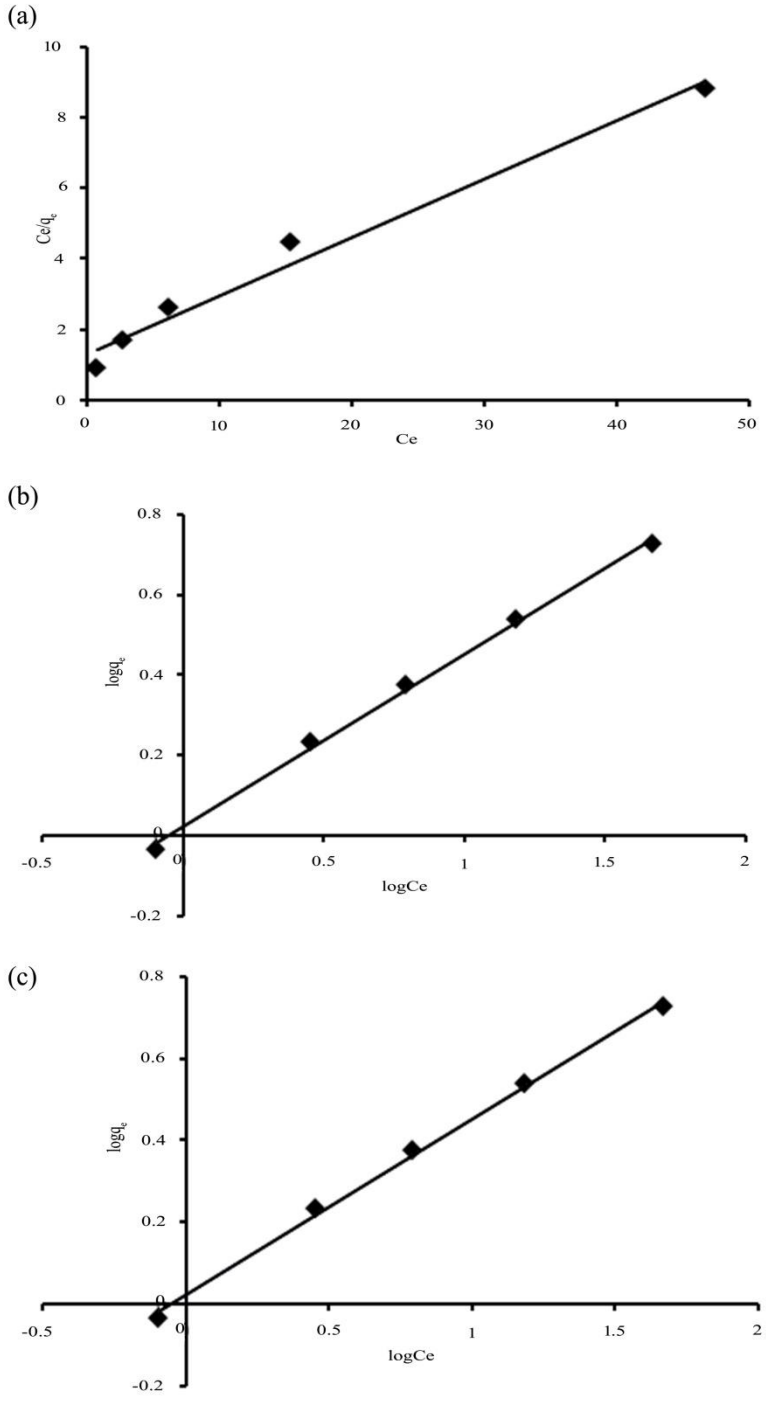

Fig. 4. Adsorption isotherm of MO onto SMBAC using different isotherm models: (a) Langmuir isotherm (b) Freundlich isotherm, and (c) Halsey isotherm.

Generally, correlation coefficient (R^2) value is used to investigate the best fitted isotherm model. In this study, three isotherm models (The Langmuir, Freundlich and Halsey) were used to determine the adsorption behavior of MO onto SMBAC (Fig. 4). The correlation coefficient (R^2) value suggests that the Freundlich and Halsey models fitted well than Langmuir model (Table 1). Freundlich and Halsey model describe the heterogonous distribution of active site with multilayer

adsorption of MO onto SMBAC. The maximum adsorption capacity of SMBAC was 6.071 mg/g (Table 1).

Table 1. Isotherm models parameters for adsorption of MO onto SMBAC.

Models	Parameters	Value
Langmuir	q_{max} (mg/g)	6.071
	b (L/mg)	0.126
	R_L	0.073-0.442
	R^2	0.979
Freundlich	K_F (mg/g) (L/mg)$^{1/n}$	1.053
	n	2.324
	R^2	0.997
Halsey	K_H	1.022
	n_H	2.324
	R^2	0.997

Langmuir parameter (R_L) values (0.073−0.442) were less than 1.0, indicating that the adsorption process of MO onto SMBAC was favorable. The higher values of n (2.324) and K_F (1.053) from the Freundlich isotherm (Table 1) suggest that the adsorption process of MO onto SMBAC from aqueous solution was suitable and easy.

The adsorption kinetics parameters give important information for designing and modeling the adsorption processes. Four kinetic models (The pseudo-first order model, pseudo-second order model, intraparticle diffusion model and Boyed model) were applied to know the adsorption kinetics of MO onto SMBAC, and presented in Fig. 5 and Table 2. According to correlation coefficient (R^2), the value of pseudo-second order kinetic model (R^2=0.999) was higher than pseudo-first order kinetic model (R^2=0.986), and the calculated $q_{e,cal}$ value of pseudo-second order kinetic model was also close to experimental $q_{e,exp}$ value (Table 2), indicating the adsorption process of MO onto SMBAC follow pseudo-second order kinetic model better.

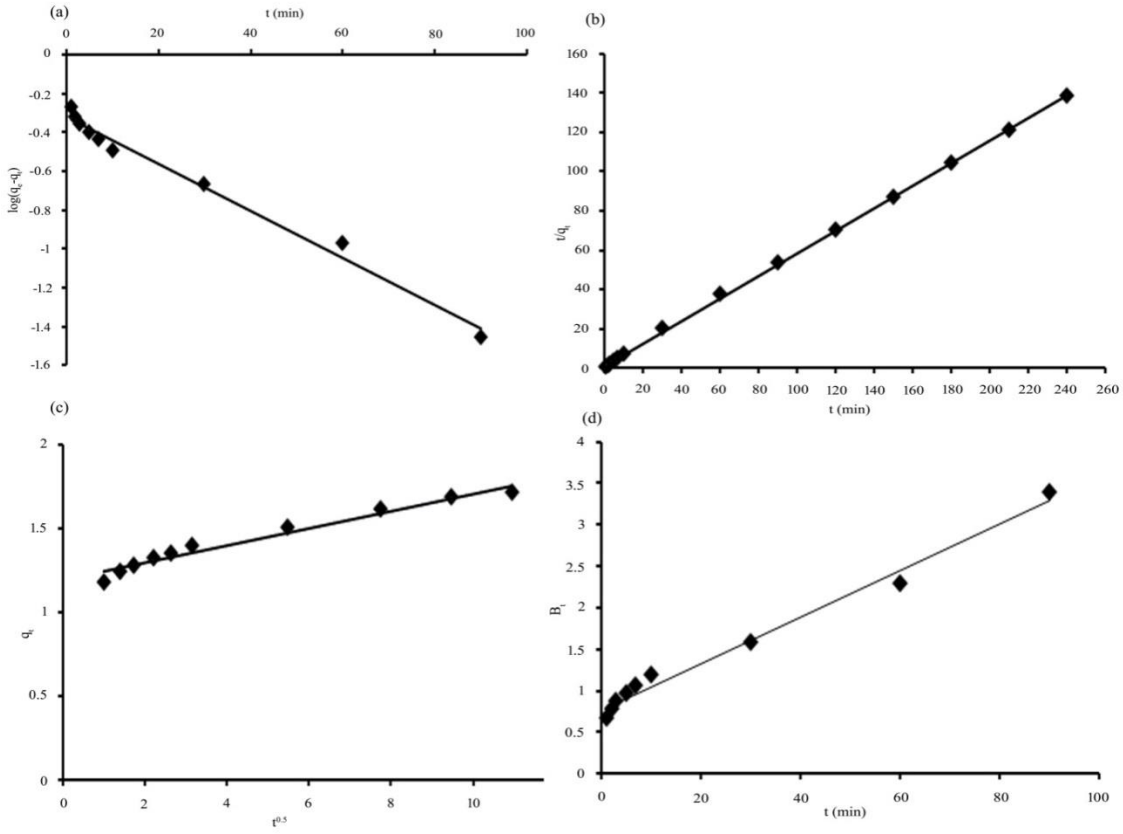

Fig. 5. Adsorption kinetic of MO onto SMBAC using different kinetic models: (a) Pseudo-first order (b) Pseudo-second order (c) Intraparticle diffusion, and (d) Boyd.

So, it confirms that the adsorption process was chemisorption, including sharing or exchange of electrons between MO and adsorbent (Bhattacharya & Sharma, 2005). Diffusion mechanisms of MO adsorption were analyzed by intraparticle diffusion model and Boyed model (Table 2). The intraparticle diffusion plot did not pass through the origin (Fig. 5(c)) due to the variation of mass transfer from initial to final stage of adsorption process (Pathania et al., 2013), and intercept (1.190) value was higher than 0.0, suggesting that not only intraparticle diffusion but multi diffusion processes (eg. firm, pore or surface diffusion) involved during adsorption of MO onto SMBAC, that may be occurred simultaneously (Kumar & Kumaran, 2005). On the other hand, the Boyed plot showed that film diffusion was the rate-limiting step for adsorption of MO onto SMBAC because the plots were linear and did not pass through the origin (Fig. 5(d)).

Table 2. Kinetic models parameters for adsorption of MO onto SMBAC.

Models	Parameters	Value
Pseudo-first order	$q_{e.exp}$ (mg/g)	1.715
	$q_{e.cal}$ (mg/g)	2.076
	K_1 (min^{-1})	0.028
	R^2	0.986
Pseudo-second order	$q_{e,exp}$ (mg/g)	1.715
	$q_{e,cal}$ (g/mg/min)	1.743
	K_2 (g/mg/min)	0.259
	H (mg/g/min)	0.789
	R^2	0.999
Intraparticle diffusion	$q_{e,exp}$ (mg/g)	1.715
	K_{diff} (mg/g $min^{0.5}$)	0.051
	C (mg/g)	1.190
	R^2	0.968
Boyd	R^2	0.986

CONCLUSION

In this study, SMBAC is a unique adsorbent prepared, characterized and applied for the removal of MO from aqueous solution by batch adsorption method. The optimum experimental conditions were achieved at pH (3) and equilibrium contact time (120 min). FTIR and SEM analysis result indicates that the surface of SMBAC contain different functional groups and active pore space. The adsorption equilibrium data well described by Freundlich and Halsey isotherm models, where Langmuir monolayer adsorption capacity was 6.071 mg/g. The adsorption kinetic curves and fitting parameters follow pseudo-second order model with multi-step diffusion process. At last, all evidences also confirm that SMBAC could be employed as a promising and low cost adsorbent to remove MO from aqueous solution or wastewater, particularly in areas without access to centralized wastewater treatment facilities.

ACKNOWLEDGEMENTS

The authors would like to extend thanks to The World Academy of Science (TWAS) for instrumental facility under the COMSTECH-TWAS Joint Research Grants Programme (TWAS Ref: 13-371 RG/ENG/AS_C; UNISCO FR: 3240279207) and KURITA Water and Environment Foundation for research grant award [17P037].

GRANT SUPPORT DETAILS

The present research has been financially supported by The World Academy of Science (TWAS) for instrumental facility under the COMSTECH-TWAS Joint Research Grants Programme (grant No. TWAS Ref: 13-371 RG/ENG/AS_C; UNISCO FR: 3240279207) and KURITA Water and Environment Foundation for research grant award (grant No.17P037).

CONFLICT OF INTEREST

The authors declare that there is not any conflict of interests regarding the publication of this manuscript. In addition, the ethical issues, including plagiarism, informed consent, misconduct, data fabrication and/ or falsification, double publication and/or submission, and redundancy has been completely observed by the authors.

LIFE SCIENCE REPORTING

No life science threat was practiced in this research.

REFERENCES

Aksu, Z. (2005). Application of biosorption for the removal of organic pollutants: a review. Process Biochem., 40(3-4); 997-1026.

Ai, L., Zhang, C. and Meng, L. (2011). Adsorption of methyl orange from aqueous solution on hydrothermal synthesized Mg–Al layered double hydroxide. J. Chem. Eng. Data., 56(11); 4217-4225.

Afroze, S., Sen, T. K. and Ang, H. M. (2016). Adsorption performance of continuous fixed bed column for the removal of methylene blue (MB) dye using *Eucalyptus sheathiana* bark biomass. Res. Chem. Intermediat., 42(3); 2343-2364.

Babel, S. and Kurniawan, T. A. (2003). Low-cost adsorbents for heavy metals uptake from contaminated water: a review. J. Hazard. Mater., 97(1-3); 219-243.

Bellifa, A., Makhlouf, M. and Boumila, Z. H. (2017). Comparative study of the adsorption of methyl orange by bentonite and activated carbon. Acta Phys. Pol. A., 132; 466-468.

Bhattacharyya, K. G. and Sharma, A. (2005). Kinetics and thermodynamics of methylene blue adsorption on neem (*Azadirachta indica*) leaf powder. Dyes Pigments., 65(1); 51-59.

Cáceres-Jensen, L., Rodríguez-Becerra, J., Parra-Rivero, J., Escudey, M., Barrientos, L. and Castro-Castillo, V. (2013). Sorption kinetics of diuron on volcanic ash derived soils. J. Hazard. Mater., 261; 602-613.

Cheah, W., Hosseini, S., Khan, M. A., Chuah, T. G. and Choong, T. S. (2013). Acid modified carbon coated monolith for methyl orange adsorption. Chem. Eng. J., 215; 747-754.

Chen, S., Zhang, J., Zhang, C., Yue, Q., Li, Y. and Li, C. (2010). Equilibrium and kinetic studies of methyl orange and methyl violet adsorption on activated carbon derived from *Phragmites australis*. Desalination., 252(1-3); 149-156.

DIM, P. E. (2013). Adsorption of methyl red and methyl orange using different tree bark powder. Adsorption., 4 (1); 330-338.

Freundlich, H. (1906). Over the Adsorption in Solution. J. Chem. Phys., 57; 358–47.

Garg, V. K., Amita, M., Kumar, R. and Gupta, R. (2004). Basic dye (methylene blue) removal from simulated wastewater by adsorption using Indian Rosewood sawdust: a timber industry waste. Dyes Pigments., 63(3); 243-250.

Garg, V. K., Kumar, R. and Gupta, R. (2004). Removal of malachite green dye from aqueous solution by adsorption using agro-industry waste: a case study of *Prosopis cineraria*. Dyes Pigments., 62(1); 1-10.

Ghasemian, E. and Palizban, Z. (2016). Comparisons of azo dye adsorptions onto activated carbon and silicon carbide nanoparticles loaded on activated carbon. Int. J. Environ. Sci. Te., 13(2); 501-512.

Gong, R., Ye, J., Dai, W., Yan, X., Hu, J., Hu, X., Li, S. and Huang, H. (2013). Adsorptive removal of methyl orange and methylene blue from aqueous solution with finger-citron-residue-based activated carbon. Ind. Eng. Chem. Res., 52(39); 14297-14303.

Gong, R., Ding, Y., Li, M., Yang, C., Liu, H. and Sun, Y. (2005). Utilization of powdered peanut hull as biosorbent for removal of anionic dyes from aqueous solution. Dyes Pigments., 64(3); 187-192.

Halim, A. A., Aziz, H. A., Johari, M. A. M. and Ariffin, K. S. (2010). Comparison study of ammonia and COD adsorption on zeolite, activated carbon and composite materials in landfill leachate treatment. Desalination., 262(1-3); 31-35.

Han, R., Zou, W., Yu, W., Cheng, S., Wang, Y. and Shi, J. (2007). Biosorption of methylene blue from aqueous solution by fallen phoenix tree's leaves. J. Hazard. Mater., 141(1); 156-162.

Haque, M. A., Khan, G. M., Razzaque, S. M., Khatun, K., Chakraborty, A. K. and Alam, M. S. (2013). Extraction of rubiadin dye from Swietenia mahagoni and its dyeing characteristics onto silk fabric using metallic mordants. Indian J. Fibre. Text. Res., 38; 280-284.

Haque, E., Jun, J. W. and Jhung, S. H. (2011). Adsorptive removal of methyl orange and methylene blue from aqueous solution with a metal-organic framework material, iron terephthalate (MOF-235). J. Hazard. Mater., 185(1); 507-511.

Ho, Y. S. and McKay, G. (2000). The kinetics of sorption of divalent metal ions onto sphagnum moss peat. Water Res., 34(3); 735-742.

Huang, J. H., Huang, K. L., Liu, S. Q., Wang, A. T. and Yan, C. (2008). Adsorption of Rhodamine B and methyl orange on a hypercrosslinked polymeric adsorbent in aqueous solution . Colloid Surf. A Physicochem. Eng. Asp., 330(1); 55-61.

Hasan, M. B. and Hammood, Z. A. (2018). Wastewater Remediation via Modified Activated Carbon: A Review. Pollution, 4(4); 707-723.

Jalil, A. A., Triwahyono, S., Adam, S. H., Rahim, N. D., Aziz, M. A. A., Hairom, N. H. H., Razali, N. A. M., Abidin, M. A. Z. and Mohamadiah, M. K. A. (2010). Adsorption of methyl orange from aqueous solution onto calcined Lapindo volcanic mud. J. Hazard. Mater., 181(1-3); 755-762.

Kumar, K. V. and Kumaran, A. (2005). Removal of methylene blue by mango seed kernel powder. Biochem. Eng. J., 27(1); 83-93.

Langmuir, I. (1917). The Constitution and Fundamental Properties of Solids and Liquids.II. Liquids. J. Am. Chem. Soc., 39(9); 1848–1906.

León, G., García, F., Miguel, B. and Bayo, J. (2016). Equilibrium, kinetic and thermodynamic studies of methyl orange removal by adsorption onto granular activated carbon. Desalin. Water Treat., 57(36); 17104-17117.

Leitch, A. E., Armstrong, P. B., and Chu, K. H. (2006). Characteristics of dye adsorption by pretreated pine bark adsorbents. Int. J. Environ. Stud., 63(1); 59-66.

Liu, L., Lin, Y., Liu, Y., Zhu, H. and He, Q. (2013). Removal of methylene blue from aqueous solutions by sewage sludge based granular activated carbon: adsorption equilibrium, kinetics, and thermodynamics. J. Chem. Eng. Data., 58(8); 2248-2253.

Malkoc, E., and Nuhoglu, Y. (2007). Determination of Kinetic and Equilibrium Parameters of the Batch Adsorption of Cr(VI) onto Waste Acorn of *Quercusith aburensis*. Chem. Eng. Process., 46 (10); 1020-1029.

Nethaji, S., Sivasamy, A. and Mandal, A. B. (2013). Adsorption isotherms, kinetics and mechanism for the adsorption of cationic and anionic dyes onto carbonaceous particles prepared from *Juglans regia* shell biomass. Int. J. Environ. Sci. Te., 10(2); 231-242.

Nasuha, N. and Hameed, B. H. (2011). Adsorption of methylene blue from aqueous solution onto NaOH-modified rejected tea. Chem. Eng. J., 166(2); 783-786.

Olajire, A. A., Giwa, A. A., and Bello, I. A. (2015). Competitive adsorption of dye species from aqueous solution onto melon husk in single and ternary dye systems. Int. J. Environ. Sci. Te., 12(3); 939-950.

Özcan, A. S. and Özcan, A. (2004). Adsorption of acid dyes from aqueous solutions onto acid-activated bentonite. J. Colloid Interface. Sci., 276(1); 39-46.

Panda, G. C., Das, S. K. and Guha, A. K. (2009). Jute stick powder as a potential biomass for the removal of congo red and rhodamine B from their aqueous solution. J. Hazard. Mater., 164(1); 374-379.

Panda, S. P., Haldar, P. K., Bera, S., Adhikary, S. and Kandar, C. C. (2010). Antidiabetic and antioxidant activity of *Swietenia mahagoni* in streptozotocin-induced diabetic rats. Pharm. Biol., 48(9); 974-979.

Pathania, D., Sharma, S. and Singh, P. (2017). Removal of methylene blue by adsorption onto activated carbon developed from *Ficus carica* bast. Arab. J. Chem., 10; 1445-1451.

Rattanapan, S., Srikram, J., and Kongsune, P. (2017). Adsorption of methyl orange on coffee grounds activated carbon. Energy Procedia., 138; 949-954.

Royer, B., Cardoso, N. F., Lima, E. C., Vaghetti, J. C., Simon, N. M., Calvete, T. and Veses, R. C. (2009). Applications of Brazilian pine-fruit shell in natural and carbonized forms as adsorbents to removal of methylene blue from aqueous solutions—Kinetic and equilibrium study. J. Hazard. Mater., 164(2-3); 1213-1222.

Saha, T. K., Bhoumik, N. C., Karmaker, S., Ahmed, M. G., Ichikawa, H. and Fukumori, Y. (2010). Adsorption of methyl orange onto chitosan from aqueous solution. J. Water Resource Prot., 2(10); 898.

Salazar-Rabago, J. J., Leyva-Ramos, R., Rivera-Utrilla, J., Ocampo-Perez, R. and Cerino-Cordova, F. J. (2017). Biosorption mechanism of Methylene Blue from aqueous solution onto White Pine (*Pinus durangensis*) sawdust: effect of operating conditions. Sustain. Environ. Res., 27(1); 32-40.

Senthil K. P., Ramakrishnan, K., Dinesh Kirupha, S., and Sivanesan, S. (2011). Thermodynamic, kinetic, and equilibrium studies on phenol removal by use of cashew nut shell. Can. J. Chem. Eng., 89(2); 284-291.

Song, C., Wu, S., Cheng, M., Tao, P., Shao, M. and Gao, G. (2014). Adsorption studies of coconut shell carbons prepared by KOH activation for removal of lead (II) from aqueous solutions. Sustainability., 6(1); 86-98.

Srivastava, V. C., Swamy, M. M., Mall, I. D., Prasad, B. and Mishra, I. M. (2006). Adsorptive removal of phenol by bagasse fly ash and activated carbon: equilibrium, kinetics and thermodynamics. Colloid Surf. A Physicochem. Eng. Asp., *272*(1-2); 89-104.

Sun, Y., Wang, G., Dong, Q., Qian, B., Meng, Y. and Qiu, J. (2014). Electrolysis removal of methyl orange dye from water by electrospun activated carbon fibers modified with carbon nanotubes. Chem. Eng. J., 253; 73-77.

Vinoth, M., Lim, H. Y., Xavier, R., Marimuthu, K., Sreeramanan, S., Rosemal, H. M. H. and Kathiresan, S. (2010). Removal of methyl orange from solutions using yam leaf fibers. Int. J. Chemtech Res., *2*(4); 1892-1900.

Wang, H., Xie, R., Zhang, J. and Zhao, J. (2018). Preparation and characterization of distillers' grain based activated carbon as low cost methylene blue adsorbent: Mass transfer and equilibrium modeling. Adv. Powder Technol., 29(1); 27-35.

Wang, J., Ma, H., Yuan, W., He, W., Wang, S. and You, J. (2014). Synthesis and characterization of an

inorganic/organic-modified bentonite and its application in methyl orange water treatment. Desalin. Water Treat., 52(40-42); 7660-7672.

Weber, W. J. and Morris, J. C. (1963). Kinetics of adsorption on carbon from solution. J. Sanit. Eng. Div., 89(2); 31-60.

Yu, J., Zhang, X., Wang, D. and Li, P. (2018). Adsorption of methyl orange dye onto biochar adsorbent prepared from chicken manure. Wat. Sci. Tech., 77(5); 1303-1312.

Zhao, P., Zhang, R. and Wang, J. (2017). Adsorption of methyl orange from aqueous solution using chitosan/diatomite composite. Wat. Sci. Tech., 75(7); 1633-1642.

Zhuannian, L. I. U., Anning, Z. H. O. U., Guirong, W. A. N. G. and Xiaoguang, Z. H. A. O. (2009). Adsorption behavior of methyl orange onto modified ultrafine coal powder. Chinese J. Chem. Eng., 17(6); 942-948.